

Experimental Study on Seismic Behavior of Seismic-damaged Lateral Joints in Composite Frame Consisting of CFSST Columns and Steel Beams Strengthened with Enclosed Reinforced Concrete

Chengxiang Xu ^{1#}, Li Zhou ¹, Kailong Xu ², Wei Peng ³

1. School of Urban Construction, Yangtze University, Jingzhou 434023, China

2. Guangdong Zhonggong Architectural Design Institute Co., Ltd, Guangzhou 510034, China

3. HNA Holding Group Co., Ltd, Haikou 570100, China

#Email: cx_xu@sina.com

Abstract

A new composite strengthening method of seismic-damaged lateral joints in composite frame consisting of Concrete-Filled Square Steel Tubes (CFSST) columns and steel beams strengthened with enclosed Reinforced Concrete (RC) at the ends of columns and welding steel plates at the ends of beams was presented. Based on the current design specifications, one half scaled models of 4 lateral joints in composite frame consisting of CFSST columns and steel beams were designed and manufactured. One model was original control specimen, one was strengthened by enclosed RC, and the others were strengthened after pre-damage. The destruction tests under lateral cyclic load on the models were carried. The effectiveness of seismic-damaged joints strengthened with enclosed RC and the reinforcement effect on different levels of seismic damage were studied. The test results show that seismic-damaged joints in composite frame consisting of CFSST columns and steel beams strengthened with enclosed RC meets the strong column-weak beam joints requirement of seismic design, and the failure modes are of all joints are the bending failure of steel beam. The reinforcement with enclosed RC has a significant on increasing the ultimate capacity and the seismic behaviors of joints. The study indicated the rehabilitated joints recover the level of their original seismic performances before seismic damage in a certain extent damage level. Based on the test data, namely the ultimate capacity, limit displacement, ductility, the energy consumption coefficient, limit displacement the strengthening method of seismic-damaged joints by strengthened with enclosed RC is an effective method for seismic strengthening.

Keywords: *Frame Joint with Concrete-Filled Square Steel Tube (CFSST)-Steel Beam; Strengthening with Enclosed Reinforced Concrete (RC); Quasi-Static Test, Seismic Damage; Seismic Behavior*

1 INTRODUCTION

Concrete-Filled Steel Tubular (CFST) structure has a good seismic performance. It has been widely used in seismic fortification area, but "Standard for seismic appraisal of buildings GB50023-2009", "Technical specification for seismic strengthening of buildings JGJ116-2009" and "Earthquake building evaluation and strengthening technical guide" were not related to the seismic identification and strengthening of CFST structures. Therefore, it is particularly urgent and important for studying the seismic strengthening of CFST structures to improve the seismic capacity and post-earthquake recovery and reconstruction [1].

Based on the current design specification, reinforced concrete frame joints have been designed and manufactured by

Lu Zhou-dao[2], Cao Zhong-min[3], Yu Jiang-tao[4] and Weng Da-gen[5]. First, pre-damage load was carried to simulate earthquake damage, then different methods (such as, fiber reinforcement method, concrete reinforcement method, enclosed steel reinforcement method and grouting repair) were used to strengthen joints. The destruction tests under low cyclic loading on joints were carried. The feasibility and effectiveness of these reinforcement methods were studied.

Enclosed concrete reinforcement method also known as increasing cross-section reinforcement method, is a method of reinforcing a structural member or structure by increasing the cross-sectional area. It can not only improve the carrying capacity of the reinforcing member, but also can increase the stiffness of the cross-section, and change the natural frequency, and make the performance of the normal use of the stage in a way to improve. This method is widely used in reinforced concrete structure's reinforcement [6].

Based on the experimental research on the seismic performance of seismic damaged CFST frame joints strengthened with CFRP, the new composite strengthening method of seismic damaged lateral joints in composite frame consisting of Concrete-Filled Square Steel Tubes (CFSST) columns and steel beams strengthened with enclosed Reinforced Concrete (RC) at the ends of columns and welding steel plate at the ends of beams was presented. Based on the current design specifications, joint models in composite frame consisting of CFSST column-steel beams were designed and manufactured, the pre-earthquake damage was simulated, earthquake damaged components were reinforced and the destruction tests under low-cycle load on the reinforcement components were carried. The ultimate capacity, limit displacement, ductility, and the energy dissipation coefficient of joints strengthened by the new composite strengthening method with different damage were studied. The effectiveness of seismic damaged CFSST frame joints based on the enclosed concrete seismic reinforcement was tested.

2 EXPERIMENTS

2.1 Specimen Design and Mechanical Properties of Materials

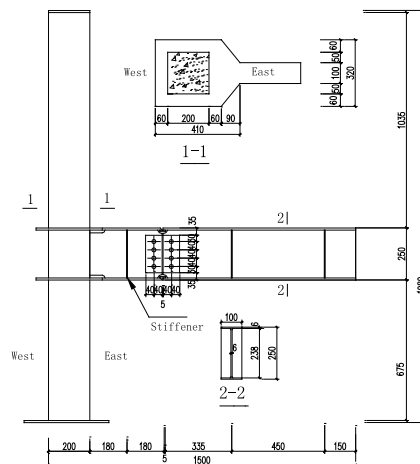


FIG.1 DIMENSION AND DETAILS OF SPECIMEN

TABLE 1 MATERIAL PROPERTIES OF STEEL

Steel Type	Thickness t/mm	Yield Strength f_y /MPa	Ultimate Strength f_u /MPa	Elasticity Modulus E_s /MPa
Steel	6	358.5	401.7	2.03×10^5
	8	385.4	458.8	1.86×10^5
	10	357.4	437.2	2.01×10^5
	12	343.1	420.1	1.88×10^5
Steel Bar	6	224.3	279.2	2.01×10^5
	12	367.6	536.4	2.01×10^5

Design principles and construction of the specimen are in reference [1]. Dimension and details of specimen are shown in Fig.1. 4 Specimens were manufactured and the core concrete in steel tube was poured at the same batch. The average

value of core concrete cube compressive strength is 46.5MPa. Specimen numbers are respectively BJDR-0, BJDR-1, BJDR-2 and BJDR-3. Based on "metallic materials-tensile at ambient testing temperature GB/T228-2002" [7], the measured mechanical properties of steel are in Table 1.

2.2 Load Test and Measurement

The loading scheme, loading systems and test content are the same as references [1]. Measuring point arrangement of strain gauge is shown in Fig.2, and Layout of displacement transducers is shown in Fig. 3.

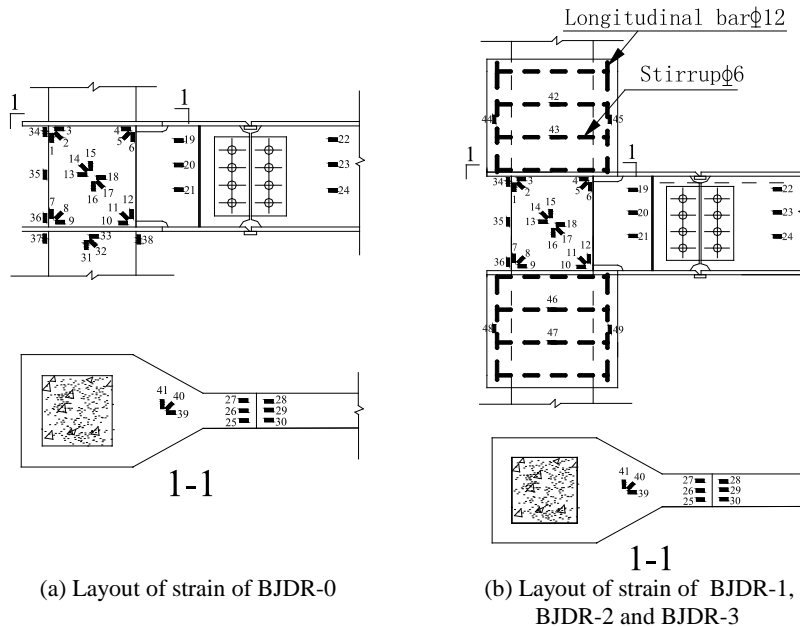


FIG.2 LAYOUT OF STRAIN GAUGES

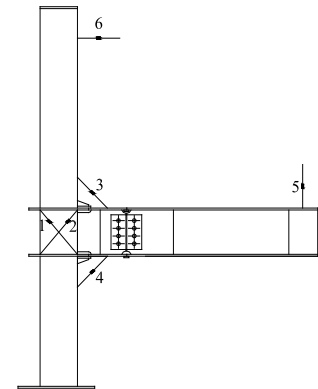


FIG.3 LAYOUT OF DISPLACEMENT TRANSUCERS

2.3 Pre-damage Specimen, Repair and Reinforcement

The pre-damage loading process of specimens is the same as the test loading process. Refer to "Earthquake building evaluation and strengthening technical guide" [8] and "Classification of earthquake damage to building and special structures" [9], the different levels of pre-damage were given. Moderate damage and severe damage of specimens in earthquake were simulated respectively.

TABLE 2 PARAMETERS OF STRENGTHENED JOINTS

No.	n	P /kN	Level of Damage	Δ /mm	Reinforcement
BJDR-0	0.3	500	No	No	No
BJDR-1	0.3	500	No	No	Yes
BJDR-2	0.3	500	Moderate	26	Yes
BJDR-3	0.3	500	Severe	33	Yes

BJDR-0 without reinforcement, as a reference specimen, was loaded directly to the destruction. BJDR-1 without pre-damage, which was strengthened by the enclosed concrete, was loaded directly to the destruction. BJDR-2 and BJDR-3 were applied by the low cyclic load to simulate earthquake action to form the pre-damage. The column end displacement was $2\Delta_y$ (26mm) and $2.5\Delta_y$ (33mm) respectively, then stop the loading and un-loading (Yield displacement Δ_y is defined as the column end displacement of BJDR-0 specimen at yield). BJDR-2 and BJDR-3 were loaded to the destruction after they were strengthened by the enclosed RC. Parameters of strengthened joints are in Table 2. In Table 2, n is axial compression ratio, P is axial force, and Δ is the column end displacement.

After the pre-damage of BJDR-2 and BJDR-3 were made, the models were repaired by welding repair, then strengthened by the enclosed reinforce. The damaged part of BJDR-1 and BJDR-2 pre-damage are mainly in the beam end, and the damage location is in the lower flange of the steel beam at bolt connection (Fig. 4). There is no significant buckling on the ring stiffener and plastic hinges appear in the outer ring plate of the beam end.



(a) Pre-damage of BJDR-2



(b) Repair of BJDR-2



(c) Pre-damage of BJDR-3



(d) Repair of BJDR-3

FIG.4 PRE-DAMAGE AND REPAIR OF BJDR-2 AND BJDR-3

Reinforcement plan:

plates reinforcement at beam end. 400mm × 20mm × 6mm Q235B steel plate is welded on the top flange and bottom flange of the beam end to increase the joint stiffness and flexural properties of the beam, and to make the plastic hinge as far as possible transfer to the ring stiffener. (Fig.5a).The ductility and energy dissipation of joints is better under the same condition, because the fracture section is closer to ring stiffener [10].

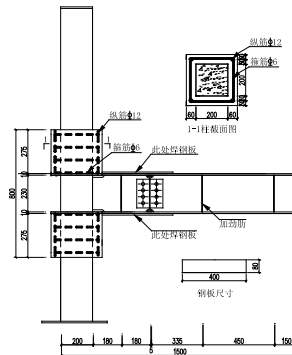
① Welding repair. Damage which occurred during p

③ Enclosed

column end. The upper and lower column is strengthened by the enclosed concrete with longitudinal reinforcement and stirrups (Fig. 5b). Measured material properties of the longitudinal reinforcement and stirrups steel are in Table 1. The average value of the cube compressive strength of the enclosed concrete is 48.4MPa. BJDR-1, BJDR-2 and BJDR-3 were strengthened by the same method. Reinforcement site is shown in Fig. 5c.



(a) Steel reinforcement at the beam end



(b) Enclosed RC at the column end



(c) Reinforcement site

FIG.5 STRENGTHENING WITH ENCLOSED RC

3 TEST PROCESS AND RESULTS

3.1 Test Description and Failure Characteristics

The vertical load is applied, check the test instruments. The horizontal load is carried after the test instruments are working properly. To describe the test phenomena easily, the assumption is made that tension of actuator loading direction is positive and thrust of actuator loading direction is negative.

Fig. 6 shows the failure characteristics of the specimen. Failure of joint specimens is at the beam end. Failure position mainly located at steel beam flange region between the ring stiffener and bolt connection. There is no significant buckling deformation on the ring stiffener.



(a) Crack at bottom flange in BJDR-0



(b) Fracture at bottom flange in BJDR-1



(c) Crack at bottom flange in BJDR-2



(e) Concrete crack at column end in BJDR-1

FIG.6 TYPICAL FAILURE MODE OF JOINTS

BJDR-0 without reinforcement was loaded directly to the destruction. The paint of top flange at the connection of steel beam bolt began to peel off when the load displacement is $\pm 15\text{mm}$ in the process of cycle. Relatively minor bulging deformation of the bottom flange appears at the connection of steel beam bolt, and the strain of the measuring point 28 to 30 located in the bottom flange of steel beam are more than the yield strain when the displacement reach at -22mm in the first cyclic loading of the load displacement $\pm 24\text{mm}$ cycle. Severe bulging deformation of the flange appears at the connection of steel beam bolt when the load displacement is $\pm 32\text{mm}$ in the process of cycle. With cyclic loading, bulging deformation alternate apparent and the beam end have significant plastic hinges. Serious bulging deformation of the steel beam appears at section change of the ring stiffener, and the small cracks began to appear at the bottom flange at the connection of steel beam bolt when the displacement reach at $+35\text{mm}$ in the third cyclic loading of the load displacement $\pm 32\text{mm}$ cycle. The bulging deformation cannot be restored when the actuator is pushed. The crack of the bottom flange at the connection of steel beam bolt increases with horizontal load in the first cyclic loading of the load displacement $\pm 42\text{mm}$ cycle. The steel beam flange fracture and the test stops when the horizontal load drops to below 85% of the ultimate load. The failure characteristics of BJDR-0 are shown in Fig. 6a.

BJDR-1 without pre-damage, which was strengthened by the enclosed concrete, was loaded directly to the destruction. Minor bulging deformation of the flange appears at the connection of steel beam bolt, and the strain of the measuring point 28 to 30 located in the bottom flange of steel beam are more than the yield strain when the displacement reach at -30mm in the first cyclic loading of the load displacement $\pm 32\text{mm}$ cycle. The concrete cracks on the south, north, east side of the upper column appear (Fig. 6d), and the bulging deformation of the steel beam flange at the bolt connection is not serious in the first cyclic loading of the load displacement $\pm 42\text{mm}$ cycle. The bulging deformation is obvious and cannot be restored when the displacement reach at -40mm in the third cyclic loading of the load displacement $\pm 42\text{mm}$ cycle. The cracks of the bottom flange appear at the connection of steel beam bolt in the first cyclic loading of the load displacement $\pm 52\text{mm}$ cycle. The cracks occur at the original steel beam, and cracks on the steel for reinforcement do not appear. The crack of the bottom flange increase and the concrete cracks of the lower column appear in the second cyclic loading of the load displacement $\pm 52\text{mm}$ cycle. The steel for reinforcement fractures and the horizontal load drops to below 85% of the ultimate load in the first cyclic loading of the load displacement $\pm 62\text{mm}$ cycle. The test stops. The failure characteristics of BJDR-1 are shown in Fig. 6b.

BJDR-2 is a specimen with moderate pre-damage and is strengthened by the enclosed concrete. Relatively minor bulging deformation of the flange, which can be recovered, appears at the connection of steel beam bolt, and the strain of the measuring point 28 to 30 located in the bottom flange of steel beam are more than the yield strain when the load displacement is $\pm 32\text{mm}$ in the process of cycle. The concrete cracks on the upper and lower column appear (The concrete cracks on the lower column mainly appear on the east side), and small cracks of the original steel beam near the web appear when the displacement reach at -32mm in the third cyclic loading of the load displacement $\pm 32\text{mm}$ cycle. The bulging deformation of the bottom flange is obvious in the first cyclic loading of the load displacement $\pm 42\text{mm}$ cycle. The bottom flange of the original steel beam fracture at the connection of steel beam bolt, and small cracks of the top flange appear in the second cyclic loading of the load displacement $\pm 42\text{mm}$ cycle (Fig. 5c). The bottom flange fracture and the horizontal load drop to below 85% of the ultimate load in the first cyclic loading of the load displacement $\pm 52\text{mm}$ cycle. The test stops.

BJDR-3 is a specimen with severe pre-damage and is strengthened by the enclosed concrete. A slight bulging deformation of the flange appears at the connection of steel beam bolt, and the strain of the measuring point 28 to 30 located in the bottom flange of steel beam are more than the yield strain in the first cyclic loading of the load displacement $\pm 32\text{mm}$ cycle. The concrete crack on the upper and lower column do not appears. The bottom flange of the original steel beam fracture at the connection of steel beam bolt in the second cyclic loading of the load displacement $\pm 32\text{mm}$ cycle. After loading the third cycles, the cracks are large. The bottom flange fracture and the bearing capacity of BJDR-3 decrease rapidly when the displacement reach at -42mm in the first cyclic loading of the load displacement $\pm 42\text{mm}$ cycle. The test stops. Similar phenomena exist in reinforced specimens BJDR-1, BJDR-2 and BJDR-3, and joint specimens show the beam end damage. Failure positions mainly locate in the ring stiffener and the flange of steel beam at the connection of steel beam bolt. No significant buckling deformation appears on the ring stiffener, and the joint core has no damage.

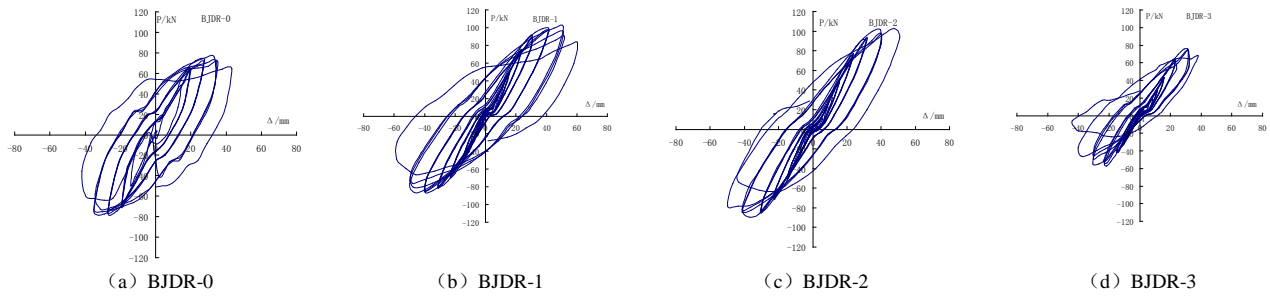


FIG.7 THE LOAD-DISPLACEMENT HYSTERETIC CURVES

3.2 Hysteretic Curves and Skeleton Curves

The horizontal load P and the displacement Δ hysteresis curve of BJDR-0, BJDR-1, BJDR-2 and BJDR-3 show in Fig.7. As can be seen.

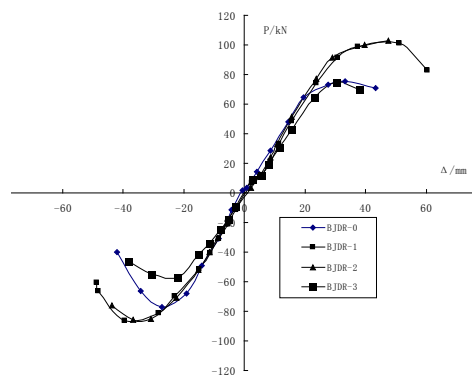


FIG.8 SKELETON CURVES OF SPECIMENS

①The hysteresis curves slope are essentially the same before yielding, and the residual deformation is small after unloading, and the hysteresis loop formed by loading and unloading are not obvious. There will be a slight slip of the curve when the loading displacement is less than 5mm, since the test conditions is limited and the actuator installation errors exist.

②The displacement magnitude at each level are 3 cycles after yielding. In the hysteresis curve of the same displacement magnitude cycle, the load value of displacement magnitude in the last two cycles is lower than the load value in first cycle. This indicates the existence of stiffness degradation. In the same displacement magnitude, the areas surrounded by hysteresis loop slightly decreases. This indicates that energy dissipation of the joint is in degradation. This degradation reflects the effect of cumulative damage of the joint.

③The load began to progressively decline with the each level displacement increasing after the peak load. With the horizontal displacement load increasing, the specimen enters the plastic development stage. Then the displacement increases rapidly, and the unloading curve is steep. Very small deformation can be recovered, and displacement lags significantly.

④Compared to BJDR-1, BJDR-2 and BJDR-3 have a certain "pinching" effect. This leads to the slightly poor plumpness.

Horizontal load - displacement skeleton curves of specimens are shown in Fig.8. The graphics are not completely symmetrical curve, because the test is affected by Bauschinger Effect and the reinforcement repair. All specimens experience elasticity, yield, limit and destruction of 4 stages under the low cyclic loading, but the yield stage is not obvious, and it shows that the yield is a diffusion process from local to the whole. Compared to BJDR-0, BJDR-1 and BJDR-2 with reinforcement have a growth of the skeleton curves. This shows that ductility of the reinforcement specimens is improved. Skeleton curves of 4 specimens are basically not much difference with little change in the stiffness before yielding, and the stiffness of BJDR-1 and BJDR-2 are significantly increased after yielding. It shows

that the enclosed reinforced concrete not only obviously improve the stiffness of the specimens, but also significantly improves the ductility of the specimens. The ultimate load and displacement of BJDR-3 is lower than the ultimate load and displacement of the other specimens. Compared with reference specimen BJDR-0, the bearing capacity and the ductility of the specimen with serious damage and reinforcement declined.

3.3 Ductility and Energy Indicators of Joints

Displacement ductility factor is calculated by the ultimate horizontal displacement Δu at the top of the column and the yield displacement Δy , as shown in Table 3.

TABLE 3 LOAD AND DISPLACEMENT OF SPECIMENS AT YIELD, ULTIMATE AND FAILURE STATE

Index No.	Loading Direction	Yield State		Damage State		Ultimate Load		μ	μ_m	h_e	E
		P_y /kN	Δy /mm	P_u /kN	Δu /kN	P_{max} /mm	Δ_{max} /mm				
BJDR-0	Positive	48.14	14.27	64.22	43.23	75.55	33.18	3.0	2.95	0.41	2.55
	Negative	47.12	12.2	65.67	35.69	77.26	29.15	2.9			
BJDR-1	Positive	55.5	18.3	82.7	60.53	101.01	51.26	3.3	3.35	0.5	3.14
	Negative	50.47	17.2	48.91	58.32	86.31	46.79	3.4			
BJDR-2	Positive	56.43	17.4	93.55	50.71	101.78	39.7	2.91	2.96	0.47	2.94
	Negative	52.03	16.5	78.02	49.94	89.79	36.70	3.0			
BJDR-3	Positive	43.11	14.55	67.75	38.03	75.62	28.93	2.6	2.82	0.38	2.4
	Negative	45.68	13.21	36.27	40.04	54.86	30.60	3.03			

BJDR-1 with the enclosed reinforced concrete is greater than reference specimen BJDR-0 in the ductility factor. The larger the specimen damage, the more ductility factor reduce. Ductility factor of BJDR-2 is less than 11.6% of ductility factor of BJDR-1, and ductility factor of BJDR-3 is less than 15.5% of ductility factor of BJDR-1. The equivalent viscous damping coefficient h_e and energy dissipation coefficient E are calculated from the load-displacement hysteresis loops of specimens, as shown in Table 3. In Table 3, μ is the ductility factor, μ_m is the mean ductility factor.

From Table 3, BJDR-0 has better energy dissipation capacity, as well as BJDR-1 and BJDR-2 with reinforcement. The main reason is that the steel beams are all the same, and the force on the ring stiffener is passed to the beam end and transition cross-section, so buckling or broken will be occurred at transition cross-section. Because of the reinforcement, compared with BJDR-0, the energy dissipation E and the equivalent viscous damping coefficient h_e of BJDR-1 are increased by 23.1% and 22.0% respectively. Compared with BJDR-0, E and h_e of BJDR-2 are increased by 15.3% and 14.6% respectively. BJDR-3 has serious damage, but is strengthened. BJDR-3 compared with BJDR-0, E and h_e is decreased by 5.9% and 7.3% respectively.

4 CONCLUSIONS

The seismic damaged load by simulated earthquake, the enclosed reinforced concrete, and the destructions tests under lateral cyclic load on the models were carried on 4 joints in composite frame consisting of CFSST columns and steel beams. The test parameters are analyzed, and the following conclusions can be drawn.

- (1) The failure features of all specimens are basically the same. The bending fracture of the specimen without reinforcement and the specimens with reinforcement occur at ring stiffener and the transition region on the steel beam, and the joint core has no damage. The strong column and weak beam stronger joints requirement of seismic design is satisfied.
- (2) The hysteretic loops of all specimens are spindle shape. Hysteretic curves of BJDR-2 and BJDR-3 with damage show "pinching" effect. Their stiffness and strength degradation is not obvious, and still has good seismic performance.
- (3) The effect of joints strengthened by the enclosed reinforced concrete is obvious. Compared with the reference specimen BJDR-0, the ultimate bearing capacity and the ductility factor of BJDR-1 with reinforcement are increased by 22.6% and 13.6% respectively. Seismic performance of BJDR-2 with moderate damage and reinforcement is similar to seismic performance of the reference specimen BJDR-0. Seismic performance of BJDR-3 with severe damage and reinforcement is slightly lower than seismic performance of the reference specimen BJDR-0.

ACKNOWLEDGEMENT

This research was funded by the National Natural Science Foundation of China (51178057) and Team of Outstanding Young Scientific and Technological Innovation of the Higher Education Institutions of Hubei Province (T201303). This support is gratefully acknowledged. The opinions expressed in this paper are those of the authors and do not necessarily reflect the opinions of the National Science Foundation of China.

REFERENCES

- [1] Xu Chengxiang, Peng Wei, Xu Kailong and Zhou Li.: Journal of Building Structures. Vol.35 (2014), P.69 (In Chinese)
- [2] Lu Zhoudao, Hong Tao and Xie Liping: Industrial Construction. Vol.33 (2003), P.9 (In Chinese)
- [3] Cao Zhongmin, Li Aiqun, Wang Yayong, Yao Qiulai: Earthquake Resistant Engineering and Retrofitting. Vol.36 (2006), P.92 (In Chinese)
- [4] Yu Jingtao, Lu Zhoudao, Zhang Kechun: Journal of Building Structures. Vol.31 (2010), P.64 (In Chinese)
- [5] Wang Dagen, Zhang Chao and Xia Jingde: China Civil Engineering Journal. Vol.46(2013), P.36 (In Chinese)
- [6] Xu Cheng-xiang, Peng Wei and Xu Kai-long: Journal of Yangtze University (Nat Sci Edit). Vol.11(2014), P.68 (In Chinese)
- [7] GB / T228.1-2010 Tensile testing of metallic materials - Part 1: Test method at room temperature. Beijing: Standard Press of China, 2011.
- [8] Ministry of Housing and Urban-Rural Development of the People's Republic of China. Earthquake Building Evaluation and Strengthening Technical Guide. Beijing: China Architecture and Building Press, 2008. (In Chinese)
- [9] Ministry of Construction of People's Republic of China. Classification of Earthquake Damage to Building and Special Structures. No. 377, 1990. (In Chinese)
- [10] Wang Wenda, Han Linhai² and You Jingtuan. China Civil Engineering Journal. Vol.39 (2006), P.17 (In Chinese)

AUTHORS



¹**Chengxiang Xu** (1965-), male, Ph.D., Professor, is mainly engaged in structural engineering.
Email: cx_xu@sina.com

²**Li Zhou** (1989-), male, Bachelor Degree, is now in graduate school, studying structural engineering
Email: zhoul20080852@163.com